Two-stream instability and oscillatory regimes induced in ballistic diodes and field-effect transistors

Z. S. Gribnikov,[a] N. Z. Vagidov, and V. V. Mitin
Department of Electrical and Computer Engineering, Wayne State University, Detroit, Michigan 48202

(Received 19 June 2000; accepted for publication 11 September 2000)

Two groups of current carriers naturally coexist in ballistic and quasiballistic diodes and field-effect transistors (FETs): (1) traversing ballistic current carriers emitted by a source and absorbed by a drain, and (2) nontraversing (nonparticipating in a current flow) carriers that are in equilibrium with the drain carrier reservoir. Therefore, the convective two-stream instability develops in such diodes and FETs with appropriate physical and geometrical parameters. It can result in oscillatory regimes. In this article, we consider development of the two-stream instability in n^+nn^+ diodes with a doped bulk *n*-base, n^+nn^+ diodes with a modulation doped *n*-channel base, and also in diodes with a gated *n*-channel base (that is in ballistic FETs) where a gate potential controls electron concentration in the channel. Since oscillatory regimes in such devices are restricted by pair electron–electron interaction between electrons belonging to the two different streams and participating in the instability process, we suggest a new type FET with two parallel *n* channels. Current-carrying electrons from the primary channel interact with slow electrons from the parallel additional channel that simultaneously serves as a controlling gate for the primary channel. In this design, electron streams participating in the two-stream instability are spatially separated, and their pair interaction is suppressed. Along with analytic estimates, we present results of numerical simulations for the ballistic FETs that prove the existence of oscillatory regimes in terahertz frequency ranges. © *2000 American Institute of Physics.* [S0021-8979(00)01224-X]

I. INTRODUCTION

Two-stream instability goes back to the well-known pioneering work of Pierce.[1] It appears both in gas discharge plasmas[1,2] and in solid state plasmas[3,4] if they contain two (or more than two) mobile components drifting with different directional velocities. In the 1960s, the two-stream instability in electron–hole plasma of bulk InSb was adjusted to the description of *K*-band coherent microwave radiation (see Refs. 5, 6 and references therein). This generation takes place in transverse magnetic fields of the Suhl configuration. Ryzhii and his co-authors[7,8] first paid attention to the two-stream instability in ballistic and quasiballistic electron transport in short-base n^+nn^+ diodes. It is known[7,9] that a bias voltage *V* across such a diode forms in its base: (1) a spatial charge region (SCR), most of which is a depletion region, and (2) a quasineutral region (QR) where negative electron charges compensate positive donor charges (see Fig. 1). A length of the SCR, x_1, is determined by voltage *V* that drops mainly across this region. A length of the QR, $l' \cong l - x_1$, is determined in the main by base length *l*. This length cannot be large because of the condition of ballisticity (or, at least, quasiballisticity) of electron transport. If this condition is well satisfied, electrons in the QR consist of two groups: (1) traversing ballistic electrons with the energy of the order of *eV* and (2) nontraversing electrons, which are in the quasiequilibrium with the drain (anode) electron reservoir. The electrons of the first group are emitted by the source (cathode) and sped up by the electric field in the SCR. We assume that the drain absorbs them without any reflection. The electrons of the second group are emitted by the drain, and these electrons come back after they reflect from the SCR (see Fig 1). If the energy *eV* substantially exceeds a Fermi energy of the base electrons, directional velocities of electrons of the above-mentioned groups are substantially different. If the parabolic dispersion relation takes place for all of the considered electron energies, concentrations of electrons of both groups in the QR are equal: $n_1 = n_2$. If nonparabolicity occurs, and the effective mass of the traversing electrons m_1 is greater than the effective mass of the nontraversing ones m_2; the number of the former exceeds the number of the latter: $n_1 > n_2$. For infinitely large (or negative) effective mass m_1 of the traversing electrons,[9] only these traversing electrons are present in the QR: $n_2 = 0$.

The two-stream instability is a result of collective plasma oscillations of both electron groups. This instability can exist if both mentioned groups really do exist and plasma oscillations exist in each of these groups. This means that plasma frequencies in both groups must be sufficiently high

$$\omega_1 \tau_1, \omega_2 \tau_2 \gg 1. \tag{1}$$

Here τ_1 and τ_2 are the times of plasma oscillation damping in these groups, and ω_1 and ω_2 are the plasma frequencies defined by the formula

$$\omega_{1,2}^2 = e^2 n_{1,2} / \kappa_D m_{1,2}, \tag{2}$$

where κ_D is the dielectric constant. An increase in concentrations $n_{1,2}$ (in order to raise the plasma frequencies $\omega_{1,2}$) intensifies electron–electron interaction between electrons of

[a]Author to whom correspondence should be addressed; electronic mail: zinovi@besm6.eng.wayne.edu

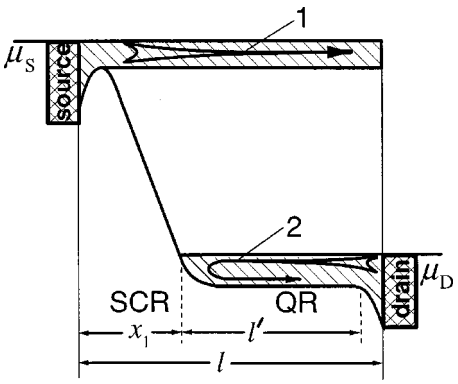

FIG. 1. Two electron streams in the quasineutral region of ballistic n^+nn^+ diode. (1) stream 1 (traversing electrons); (2) stream 2 (nontraversing electrons).

different groups. This interaction does not cancel ballistic transport on the whole. But the strong intergroup electron–electron scattering cancels the existence of the two streams and, as a result, the two-stream instability. To avoid destruction of the two-stream structure of an electron distribution function, the strong inequality

$$l'/v_1 \ll \tau_{12} \tag{3}$$

must be satisfied, where τ_{12} is the above-mentioned intergroup scattering time for the first group of electrons, and v_1 is the velocity of these traversing electrons; $v_1=\sqrt{2eV/m_1}$ for the parabolic dispersion case. Since the time τ_{12} decreases with increasing n_2 (while the time τ_{21} of scattering the second group electrons on the first group electrons decreases with increasing n_1), we cannot build up these concentrations without hindrance.

The considered two-stream instability occurs for comparatively small values of the product kv_1 (of wave number $k=|\mathbf{k}|$ into velocity v_1) and, as a result, can be implemented in sufficiently long-base samples ($l\approx\pi/k_{\max}$) at sufficiently low voltages V. To increase the real values of $k_{\max}$, to shorten the base lengths, and to raise voltage V (in order to upconvert frequencies), we need to increase donor concentrations in bulk bases. This leads to undesirable additional electron scattering by ionized donors. To avoid this effect, planar channel bases with modulation doping can be used, instead of bulk bases. The special gate potential can produce electrons in such channel bases if these bases are gated. In fact, these gated channel base diodes are field-effect transistors (FETs). As it is well known, a drain current in ballistic FETs (as in ordinary nonballistic FETs) is saturated due to the gate effect for high values of $V>V_s$, where V_s is the saturation voltage, and only traversing ballistic electrons remain in the current channel at the saturated regime. Therefore the two-stream instability is impossible under the saturation, but it is possible at $V<V_s$ (as it was predicted in Refs. 10 and 11). The saturation threshold V_s also can be increased by enhancement of electron concentration in the channel, but this enhancement is restricted by the intergroup electron–electron interaction as before.

The two-stream instability in wide ranges of voltages and concentrations can be obtained using two-channel (or, in more generalized case, multichannel) transistors instead of those with a single gated channel. A two-channel transistor contains an additional parallel ballistic channel alongside the main current-conducting ballistic channel. These channels are independently contacted. Therefore, voltages dropped across these channels are different, and electron velocities in the QRs in both channels are also different. Two-stream instability appears in this case due to electrostatic interaction of plasma oscillations in the neighboring channels. There are two advantages of the two-channel transistors over the single-channel prototypes. (1) The current saturation (and existence of only hot traversing electrons) in the main channel does not exclude development of two-stream instability due to the presence of the parallel second channel with quasiequilibrium (standing or slowly moving) electrons. This second channel is specially formed to carry the second electron stream with $v_2\approx 0$. (2) Due to the spatial separation of the streams in both channels, we can attenuate pair collisions between electrons belonging to different channels (that is, intergroup electron–electron interaction) and not attenuate interchannel interaction between plasma excitations with small values of k. As a result, we can avoid undesirable electron mixing in the momentum space.

In this article, we obtain dispersion relations $\omega(k)$ for excitations of quasineutral plasma, which consists of two electron streams in the base QR of the ballistic n^+nn^+ diode. We consider the following versions: (1) a homogeneously doped bulk n base; (2) a modulation doped planar channel n base; (3) a gated channel (transistor) n base; and, (4) a two-channel base with independently contacted and supplied channels. In the fourth case, one of the channels serves as a current-conducting base, and the other channel serves as a gate, participating in formation of the two-stream instability and simultaneously controlling a conductivity of the first channel. In all of these cases we find ranges of existence of two-stream instability and its increments.

Real finite size (short) bases of ballistic n^+nn^+ diodes and transistors limited by n^+ contacts (and gates in the transistors) are in fact certain microcavities for two-stream plasma oscillations. These cavities select the most appropriate oscillatory modes and globalize for them the initial convective instability. As a result, oscillations of diode or transistor currents appear with a certain frequency or a certain spectral composition. We consider these oscillatory regimes on the basis of the self-consistent solution of a ballistic kinetic equation in the base (bulk, channel, and two-channel structure) together with a Poisson equation in the same base and in its vicinity. We show that the ballistic diodes and FETs, with the bases of the above-mentioned types, can be oscillation generators, and generated frequencies move into a terahertz range with base shortening and carrier concentration increasing.

II. DISPERSION RELATIONS FOR BULK AND UNGATED CHANNEL BASES

A. Homogeneous bulk bases

We consider a homogeneously doped neutral bulk region with only two types of electrons: (1) electrons with the mo-

mentum p_1 directed along the x axis and with the corresponding energy $\varepsilon_1=\varepsilon(p_1)$ and velocity $v_1=v(p_1)=d\varepsilon/dp|_{p=p_1}$, and (2) electrons with the momentum $p_2\approx 0$ and correspondingly $\varepsilon_2\approx 0$ and $v_2\approx 0$. The neutrality of the base means that the sum of electron concentrations is constant,

$$n_1+n_2=n_D, \tag{4}$$

where n_D is the concentration of ionized donors, and the electric field is absent

$$E=-dV/dx=0, \tag{5}$$

where $V(x)$ is the electric potential. In this region there is the electric current with density

$$j=j_1=-ev_1n_1 \tag{6}$$

since $j_2\approx 0$. The above-described two-stream presentation of the electron distribution function is legitimate if the real spread of velocities and energies is small in comparison with the velocity v_1 and energy ε_1, respectively. At least the condition $\varepsilon_1\cong eV\gg\mu$, where μ is the Fermi energy in the QR must be satisfied.

We present small nonstationary variations of concentrations and other variables in the form of their Fourier components with the wave number k:

$$n'_{1,2}=n'_{1,2}(k)e^{ikx-i\omega(k)t} \tag{7}$$

and so on. Generally speaking, the frequencies $\omega(k)$ are complex numbers at real wave numbers k. We write out the equations defining these primed values:

the Poisson equation

$$\kappa_D k^2V'(k)=e[n'_1(k)+n'_2(k)], \tag{8}$$

the equations of continuity of the streams

$$n_1kp'_1(k)/m_1=[kv_1-\omega(k)]n'_1(k), \tag{9}$$

$$n_2kp'_2(k)/m_2=-\omega(k)n'_2(k), \tag{10}$$

and the Newton equations

$$[kv_1-\omega(k)]p'_1(k)=ekV'(k), \tag{11}$$

$$-\omega(k)p'_2(k)=ekV'(k). \tag{12}$$

To obtain Eqs. (8)–(12) we use the relations $j'_1(k)=-ev'_1(k)n_1-ev_1n'_1(k)$; $j'_2(k)=-ev'_2(k)n_2$; $v'_1(k)=d^2\varepsilon/dp^2|_{p=p_1}\cdot p'_1(k)=p'_1(k)/m(p_1)$; $v'_2(k)=p'_2(k)/m(0)$; $E'(k)=-ikV'(k)$; $m_1=m(p_1)$; $m_2=m(0)$. The dispersion relation $\omega(k)$ that follows from Eqs. (8)–(12) has the well-known form[12]

$$\frac{\omega_1^2}{(\omega(k)-kv)^2}+\frac{\omega_2^2}{\omega^2(k)}=1, \tag{13}$$

where $v=v_1$ and $\omega_{1,2}$ are defined by Eq. (2).

In the simplest and very important case of parabolic dispersion relation of electrons $\varepsilon(p)=p^2/2m$, we have $m_1=m_2$ and simultaneously $n_1=n_2=n_D/2$ in the QR (as it is shown, for example, in Refs. 9 and 13). Then, $\omega_1^2=\omega_2^2=\omega_0^2/2$, where $\omega_0^2=e^2n_D/\kappa_Dm$, and the roots of Eq. (13) are written in the form

$$\omega_{(1,2,3,4)}(k)=(1/2)\{kv\pm[k^2v^2+2\omega_0^2\pm 2(\omega_0^4+2k^2v^2\omega_0^2)^{1/2}]^{1/2}\}. \tag{14}$$

The instability occurs if $k^2v^2+2\omega_0^2<2(\omega_0^4+2k^2v^2\omega_0^2)^{1/2}$, that is

$$|kv|<2\omega_0. \tag{15}$$

Note that this instability is always convective.[12] The maximal increment takes place at $|kv|=\sqrt{3/2}\omega_0$ and is equal to $\omega_0/2\sqrt{2}$. If we assume that the longest wave mode allowed by the n base is the mode with $k_{\max}=2\pi/l'$, condition (15) transforms into $v<l'\omega_0/\pi$ and

$$V<en_Dl'^2/2\kappa_D\pi^2\equiv V_{\rm th}. \tag{16}$$

We can estimate the range of $V_{\rm th}$. If $n_D=4\times 10^{16}$ cm^{-3}, $l'=10^{-5}$ cm, and $\kappa_D=12/(4\pi)$, then we obtain $V_{\rm th}\cong$ 30 mV. Increase in $V_{\rm th}$ by increasing l' is limited because of the necessity of ballistic (or, at least, quasiballistic) transport. The same reason does not allow us to raise n_D (because of ionized-donor scattering and intergroup electron–electron scattering). We note that $V_{\rm th}$ does not depend on an electron effective mass. The oscillation frequency attained in the considered specific case is equal to $f=kv/2(2\pi)\leqslant\omega_0/2\pi\approx 1.5$ THz, for the electron effective mass $m=0.067m_0$ (where m_0 is the free electron mass).

Formula (13) also shows that the instability does not exist in the single component plasma consisting of only hot ballistic carriers ($n_2=0$, $n_1=n_D$) where $\omega_{(1,2)}(k)=kv\pm\omega_1(p_1)$. However, the situation changes substantially if the effective mass $(\partial^2\varepsilon/\partial p^2)^{-1}_{p=p_1}$ of the hot ballistic carriers becomes negative. Then an increment of the rising plasma oscillations appears instead of their frequency

$$\omega_{(1,2)}(k)=kv\pm i|\omega_1(p_1)|. \tag{17}$$

This case is considered in detail in a number of our group articles beginning from Ref. 9 (see Refs. 13 and 14). These oscillations increase with the same high increment for all of the values of k. Therefore, the selection of the fundamental mode is determined by correlation between x_1 and $l'\cong l-x_1$, boundary conditions, and an external load. Since the instability appears in a single stream, the role of the intergroup electron–electron scattering becomes less crucial.

B. Ungated *n* channel base

For a single ballistic n channel placed in a dielectric medium, the dispersion equation of two-stream plasma oscillations (in the limit of the very long QR) has the form

$$\frac{g_1}{(\omega(k)-vk)^2}+\frac{g_2}{\omega^2(k)}=\frac{1}{|k|}, \tag{18}$$

where $g_1=g_1(p_1)=e^2N_1/2\kappa_Dm(p_1)$, $g_2=g_2(0)=e^2N_2/2\kappa_Dm(0)$, $v=v_1=v(p_1)$, where N_1 and N_2 are the sheet concentrations (cm^{-2}) of electrons of the first and second groups (i.e., traversing and nontraversing). Equation (18) is derived in Sec. III as the limiting case of the dispersion equation for the gated channels. This equation relates by the same token both to nonquantized three dimensional (3D) channel electrons and to the limiting quantum case when all

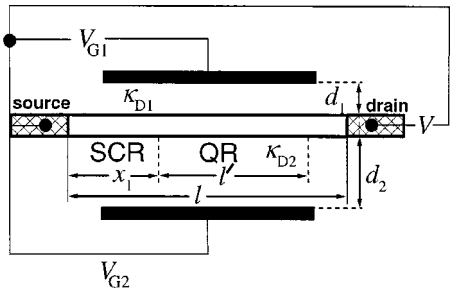

FIG. 2. Current channel between the gates of the gated n^+nn^+ diode.

of the electrons are in the lowest subband of size quantization. Equation (18) transforms into Eq. (13) as a result of the replacements, $g_{1,2}|k|=\omega_{1,2}^2$. For the parabolic dispersion relation of the channel electrons ($m_1=m_2=m$) we have, as in the case of the bulk base, $N_1=N_2=N_D/2$, where N_D is the total sheet electron concentration, and $g_1=g_2=g_0/2$, where $g_0=e^2N_D/2\kappa_D m$. Then we obtain

$$\omega_{(1,2,3,4)}(k)=(1/2)\{kv\pm[|k|(|k|v^2+2g_0 \pm 2(g_0^2+2g_0|k|v^2)^{1/2})]^{1/2}\}. \tag{19}$$

The instability occurs at $|k|v^2<4g_0$. The maximal increment appears for $|k|=(1+\sqrt{2})g_0/v^2$. It is equal to $g_0/2v$. As in the previous case, we estimate the limiting size of the longest wave mode as $k=2\pi/l'$. Thus, $v^2<2g_0l'/\pi$ and

$$V\leqslant eN_Dl'/2\pi\kappa_D\equiv V_{\rm th}. \tag{20}$$

For $N_D=2\times10^{11}$ cm^{-2}, $l'=10^{-5}$ cm, and $\kappa_D=12/(4\pi)$, we obtain $V_{\rm th}=50$ mV. The oscillation frequency decreases with an increase in the base length and increases with an increase in the concentration: $f=e(N_D/4\pi\kappa_D ml')^{1/2}$. It is equal to $\sim$2.6 THz for the aforementioned parameters and $m=0.067m_0$.

III. DISPERSION RELATIONS FOR GATED CHANNELS

A. General consideration

In this section we consider a gated n channel. Metallic gates G_1 and G_2 are placed on both sides of the channel and are isolated from the channel by dielectric barriers of widths d_1 and d_2 (Fig. 2). Generally speaking, gate potentials V_{G1} and V_{G2} differ from the potential V of the channel QR. This means that there exist some voltages $V_{G1,2}-V$ across the dielectric barriers, which enhance or deplete the channel QR. Due to the gate action, current–voltage (I-V) characteristics of the gated and ungated channels differ substantially from each other. In the bulk base and in the ungated channel a ballistic current never saturates (for a parabolic electron dispersion relation) and increases with V as $\sqrt{V}$. For the bulk base, we obtain $|j|\cong en_D\sqrt{eV/2m}$. For the ungated channel, we must replace $|j|$ by $|J|$ and n_D by N_D in this formula, where J is the sheet current density in A cm^{-1}. With increasing V, the gated channel becomes depleted more and more because of negative differences $V_{G1,2}-V$. Therefore, the electron concentration in the QR decreases, but it decreases only in the part of the nontraversing electrons, whose role in the channel is passive. The traversing electrons are current conducting, and their concentration in the QR must always be finite. As a result, the current saturates at a finite value of voltage $V=V_s$, with a finite concentration of traversing electrons N_1, and with zero nontraversing concentration $N_2=0$. In the saturated state of the gated QR, we deal with single-stream plasma. For $V>V_s$, the voltage excess $V-V_s$ drops across the new depletion region (the SCR-2) near the drain. Since $N_2=0$ at the saturation, the two-stream instability is possible only for $V<V_s$. To determine concentrations N_1 and N_2, which are not equal to each other in the gated QR, we have to solve a 2D Poisson equation in the space between gates G_1 and G_2. We assume that the channel width is negligibly small in comparison with the widths d_1 and d_2 of the top and bottom dielectric barriers having the dielectric constants κ_{D1} and κ_{D2}, respectively (Fig. 2). The Poisson equation

$$\frac{\partial E_x}{\partial x}+\frac{\partial E_y}{\partial y}=(e/\kappa_{Di})(N_D-N)\,\delta(y), \quad i=1,2 \tag{21}$$

is solved in the SCR with the length x_1, where the entire voltage $V\cong V(x_1)$ drops. In the SCR there exist only the traversing electrons, that is $N=N_1$. The concentration N_D in Eq. (21) determines the channel electron concentration, if $V_{G1,2}-V=0$. If a strong inequality,

$$x_1\gg d_{1,2}, \tag{22}$$

occurs, a potential distribution in the barriers is almost one dimensional, and we can write: $E_x\cong E_x(0)(d_1-y)/d_1$ for $d_1>y>0$ and $E_x\cong E_x(0)(d_2+y)/d_2$ for $0>y>-d_2$, where $E_x(0)$ is the channel electric field ($y=0$). As a result of integration of both sides of Eq. (21) from $-d_2$ to d_1, we obtain

$$\frac{1}{2}(\kappa_{D1}d_1+\kappa_{D2}d_2)\frac{dE_x(0)}{dx} =e(N_D-N_1(x))+\frac{\kappa_{D1}}{d_1}(V_{G1}-V(x)) +\frac{\kappa_{D2}}{d_2}(V_{G2}-V(x)). \tag{23}$$

Taking into account that $J=-ev(p)N_1$ analogously to Eq. (6), $p=p(x)$, $v(p)(dp/dx)=-eE_x(0)=e(dV(x)/dx)$, and $\varepsilon(p)=eV(p)=eV(x)$, we rewrite Eq. (23) in the form

$$\frac{e}{2}(\kappa_{D1}d_1+\kappa_{D2}d_2)E_x(0)\frac{dE_x(0)}{dx} =|J|-eN_D^*v(p)\left(1-2\frac{\varepsilon(p)}{\varepsilon_A}\right), \tag{24}$$

where $N_D^*=N_D+(\kappa_{D1}V_{G1}/ed_1)+(\kappa_{D2}V_{G2}/ed_2)$, and $\varepsilon_A=2e^2N_D^*/[(\kappa_{D1}/d_1)+(\kappa_{D2}/d_2)]$. Since the field $E_x(0)$ is equal to zero in both the effective cathode ($x\approx0$) and the

border between the SCR and the QR, $x=x_1$, we obtain $|J|p_1=eN_D^*\varepsilon(p_1)(1-\varepsilon(p_1)/\varepsilon_A)$ [as a result of integration of Eq. (24) between the limits $p(0)=0$ and $p(x_1)=p_1$], and

$$N_1=N_D^*\frac{\varepsilon(p_1)}{p_1v(p_1)}\left(1-\frac{\varepsilon(p_1)}{\varepsilon_A}\right). \tag{25}$$

On the other hand, since in the QR $E_x(0)=0$, $V(x)=V(x_1)=\varepsilon(p_1)/e$, and $N=N_1+N_2$, we obtain $N=N_D^*(1-2\varepsilon(p)/\varepsilon_A)$ [from Eq. (23) with N instead of N_1 on the right-hand side]; that is

$$N_1/N=\frac{\varepsilon(p_1)}{p_1v(p_1)}\cdot\frac{1-\varepsilon(p_1)/\varepsilon_A}{1-2\varepsilon(p_1)/\varepsilon_A}, \tag{26}$$

$$N_2/N=\frac{1-\varepsilon(p_1)/p_1v(p_1)-(\varepsilon(p_1)/\varepsilon_A)(2-\varepsilon(p_1)/p_1v(p_1))}{1-2\varepsilon(p_1)/\varepsilon_A}. \tag{27}$$

Until now, we have not specified the dispersion relation $\varepsilon(p_1)$ anywhere in this section. For the parabolic dispersion relation, formulas (26) and (27) are simplified:

$$N_1/N=\frac{1}{2}\cdot\frac{1-\varepsilon(p_1)/\varepsilon_A}{1-2\varepsilon(p_1)/\varepsilon_A};$$

$$N_2/N=\frac{1}{2}\cdot\frac{1-3\varepsilon(p_1)/\varepsilon_A}{1-2\varepsilon(p_1)/\varepsilon_A}. \tag{28}$$

In this case the current is saturated at $N_2=0$; that is at $\varepsilon(p_1)=\varepsilon_s=\varepsilon_A/3$.

In the symmetric two-gate case, when $d_1=d_2=d$, $\kappa_{D1}=\kappa_{D2}=\kappa_D$, and $V_{G1}=V_{G2}=V_G$, we obtain $N_D^*=N_D+2\kappa_DV_G/ed$; $\varepsilon_A=e^2N_Dd/\kappa_D+2eV_G$; $\varepsilon_s=eV_s=e^2N_Dd/3\kappa_D+2eV_G/3$. The saturated current density is equal to

$$J_s=\frac{4}{3\sqrt{3}}\frac{\kappa_D}{d}\left(\frac{e}{m}\right)^{1/2}(V_1^*)^{2/3},$$

where $V_1^*=\varepsilon_A/2e=V_G+eN_Dd/2\kappa_D$.

In the limiting single-gate case when $d_1=d$, $\kappa_{D1}=\kappa_D$, $V_{G1}=V_G$, and $d_2\to\infty$, we obtain $N_D^*=N_D+\kappa_DV_G/ed$; $\varepsilon_A=2e^2N_Dd/\kappa_D+2eV_G$; $\varepsilon_seV_s=2e^2N_Dd/3\kappa_D+2eV_G/3$. The saturated current density is equal to

$$J_s=\frac{2}{3\sqrt{3}}\frac{\kappa_D}{d}\left(\frac{e}{m}\right)^{1/2}(V_2^*)^{2/3},$$

where $V_2^*=\varepsilon_A/2e=V_G+eN_Dd/\kappa_D$.

Now we go to the dispersion equation for the two-stream plasma oscillations in the two-gate channel structure shown in Fig. 2. We present small nonstationary variations of concentrations and other variables in the form analogous to Eq. (7), and obtain the Poisson equation in the barriers in the form

$$\kappa_{Di}\left(\frac{1}{k^2}\frac{d^2V'}{dy^2}-V'\right)=-V'(0)\,\delta(y)\left(\frac{\hat{g}_1(p_1)}{(\omega(k)-kv)^2}+\frac{\hat{g}_2(0)}{\omega^2(k)}\right),\quad i=1,2, \tag{29}$$

where $\hat{g}_1(p_1)=e^2N_1/m_1$, $\hat{g}_2(0)=e^2N_2/m_2$, $v=v(p_1)$. Equation (29) should be solved with the boundary conditions $V'(d_1)=V'(-d_2)=0$. The resulting dispersion equation has the form

$$\frac{\hat{g}_1}{(\omega(k)-kv)^2}+\frac{\hat{g}_2}{\omega^2(k)}=(\kappa_{D1}\tanh^{-1}kd_1+\kappa_{D2}\tanh^{-1}kd_2)/k. \tag{30}$$

For the symmetric two-gate design ($d_1=d_2=d$, $\kappa_{D1}=\kappa_{D2}=\kappa_D$), Eq. (30) is simplified to the form

$$\frac{g_1}{(\omega(k)-kv)^2}+\frac{g_2}{\omega^2(k)}=\frac{1}{k\tanh kd}, \tag{31}$$

where $g_{1,2}$ are the same as in Eq. (18). For the limiting asymmetric singlegate design ($d_1=d$, $\kappa_{D1}=\kappa_D$, and $d_2\to\infty$), we obtain the equation

$$\frac{g_1}{(\omega(k)-kv)^2}+\frac{g_2}{\omega^2(k)}=\frac{1}{2k\tanh kd}+\frac{\kappa_{D2}}{2\kappa_{D1}|k|}, \tag{32}$$

which directly transforms into Eq. (18), if $\kappa_{D2}=\kappa_D$ and $d\to\infty$.

If values of d are finite, we must substitute the realistic values of $N_{1,2}$ into the expressions of g_1 and g_2. Recall that $N_{1,2}$ are now not equal to each other even for the parabolic dispersion relation and are dependent on $V_{G1,2}$ and V in the QR.

B. Symmetric two-gate FET

Taking into account formulas (28) we can obtain Eq. (31) for the parabolic dispersion relation in the form

$$(\omega(k)-kv)^{-2}+\omega^{-2}(k)+\zeta((\omega(k)-kv)^{-2}-\omega^{-2}(k))=2/gk\tanh kd, \tag{33}$$

where $\zeta=eV/(\varepsilon_A-2eV)=V/2(V_1^*-V)$ and, as above, $V_1^*=V_G+edN_D/2\kappa_D$, $eV=\varepsilon(p_1)$, and $g=e^2N/2\kappa_Dm$. We can see that $0\leqslant\zeta\leqslant1$. The current saturation takes place at $\zeta=1$. Equation (33) can be rewritten in a simpler form if we introduce the new variable,

$$\xi=\frac{\omega(k)}{kv}-\frac{1}{2},$$

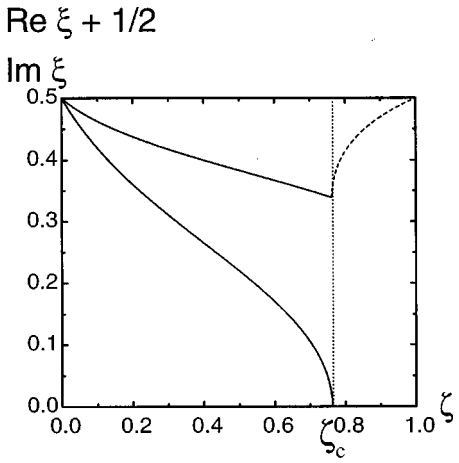

FIG. 3. The real and imaginary parts of the complex roots of Eq. (34). Upper curve (1) $\mathrm{Re}\xi+\frac{1}{2}$; lower curve (2) $\mathrm{Im}\xi$.

and take into account that $g/v^2=1/4\zeta d$. Then we obtain

$$\xi^4-\frac{1}{2}\left(1+\frac{1}{2\zeta^*}\right)\xi^2-\frac{1}{4}\frac{\zeta}{\zeta^*}\xi+\frac{1}{16}\left(1-\frac{1}{\zeta^*}\right)=0, \qquad (34)$$

where $\zeta^*=\zeta kd/\tanh kd$. In the actual case $kd\ll 1$, we have $\zeta^*\cong\zeta$. In this case, the roots of Eq. (34) depend only on the parameter ζ, and any dependence on k disappears from Eq. (34). There exists the critical value of this parameter, $\zeta_C\approx 0.767$, which separates stable and unstable states of the considered FET. The instability for $kd\ll 1$ occurs only at $\zeta<\zeta_C$, that is, for $V<V_C=2\zeta_C V_1^*/(1+2\zeta_C)\cong 0.6V_G^*$. The oscillation frequency rises proportionally to $\sqrt{V_1^*}$ with increasing V_1^*. Therefore, we obtain the additional possibility to tune this frequency in wide ranges. The dependence of real and imaginary parts of complex roots of Eq. (34) on ζ for $kd\ll 1$ is shown in Fig. 3. We can see for ourselves that an oscillation frequency (for a given value of k) depends on ζ insignificantly. But unlike the bulk base case (Sec. II A) presented by the dispersion Eq. (13), the instability in this case is not convective but absolute. To show that, we rewrite Eq. (33) with the new designations $\Omega=\omega d/v$ and $\kappa=kd$

$$\frac{1+\zeta}{(\Omega-\kappa)^2}+\frac{1-\zeta}{\Omega^2}=\frac{8\zeta}{\kappa\tanh\kappa} \qquad (33')$$

and find its roots $\kappa=\kappa(\Omega)$ for $\mathrm{Im}\,\Omega=\Omega''\to\infty$. At $\Omega'=\mathrm{Re}\,\Omega=0$, these roots are on the imaginary axis of the κ-plane ($\kappa=i\kappa''$) and tend to the values $\kappa''=\pm\pi/2$, $\pm 3\pi/2,\ldots$. With decreasing Ω'' these roots tend to $\kappa''=0$ from both sides and block any possible shifts of the integration contour, which initially coincided with the real axis. This behavior of the contour is known to be a criterion of the absolute instability.[12,15]

We will show in Sec. V that the above-mentioned absolute instability leads to stratification of the electron concentration in the current-conducting channel with forming quasiperiodic distribution along the current direction. If distances d are sufficiently small, this stratification does not impede the development of quasiconvective instability in the stratified structure and the consequent appearance of current oscillation regimes.

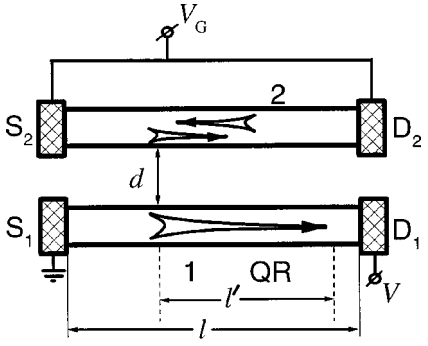

FIG. 4. Two-channel design of the n^+nn^+-ballistic FET.

C. Asymmetric single-gate FET

For the parabolic dispersion relation, Eq. (32) can be obtained from Eq. (33) as a result of replacement: $2/gk\tanh kd\to(1/g)[(1/k\tanh kd)+1/|k|]$ with $\zeta=V/2(V_2^*-V)$ and $V_2^*=V_G+edN_D/\kappa_D$. Taking into account that in this case $g/v^2=1/8\zeta d$, we can reduce the so transformed equation to the form of Eq. (34) with replacement of ζ^* by $\zeta^{**}=\zeta kd(1+\tanh|k|d)/\tanh kd$. For $kd\ll 1$, we have $\zeta^{**}\cong\zeta$, and the asymmetric FET case is reduced to the previous case of the symmetric FET.

IV. TWO-STREAM INSTABILITY IN PARALLEL CHANNELS

Up to now, we have exploited the mechanism of the two-stream instability based on different behavior of ballistic electrons emitted by the cathode and anode. The former, which are the traversing electrons, gain a sufficiently high velocity in the SCR, while the latter can be considered completely immobile. We have assumed that ballistic electrons interact very weakly not only with phonons, impurities, and imperfections but also with each other. That is, we have assumed that each of two above-mentioned electron groups moves independently. Numerous investigations of electron–electron interaction in bulk samples (see Ref. 16 and references therein) and in 2D electron-gas samples[17–22] show that we can count on large times τ_{12} of intergroup interaction only in the cases of: (1) low electron concentrations, and (2) low voltages V in the QR (and correspondingly small energies of traversing electrons). To avoid this strong interaction, we must spatially separate the above-mentioned two electron groups (similar to separation of electrons in the channels and donors in the barriers in modulation-doped structures). The electron–electron interaction between the carriers in parallel current channels was studied in due time very intensively both theoretically[23–25] and experimentally.[26–28] The devices that were considered in these works are just the two-channel FETs (with the exception of the transport ballisticity in the channels). The ''theoretical'' dependence of interchannel momentum scattering time τ_D on the distance d (see Fig. 4) is $\tau_D^{-1}\sim d^{-4}$. For $d\approx 20$ nm, $\tau_D\approx\tau_\mu/1000$, where τ_μ is the relaxation time defining electron mobilities in the channels[28] (that is, there are $\tau_D^{-1}\cong 10^7-10^8\ \mathrm{s}^{-1}$ for liquid helium temperatures).

The above-mentioned separation allows us to exploit a working regime when only (or mainly) traversing electrons are present in the current-conducting channel 1 (Fig. 4). This regime is a saturation regime. The second electron stream (of nontraversing electrons) is suggested to take place in the additional parallel channel 2 having some potential relative to the QR of channel 1. We need to select this potential so that the electron concentrations in the channels N_1 and N_2 are approximately equal to each other in the saturation regime. The distance between the channels must be much smaller than the QR length l' in order to develop the two-stream instability with participation of electrons of both channels. Each of the channels contains only one of the two participating streams. A summary doping determines a summary concentration of electrons N_1+N_2, while the potential of channel 2 redistributes these electrons between the channels. That is, channel 2 simultaneously plays two roles: (1) the container of the second electron stream, and (2) the controlling gate.

The simplest dispersion equation describing the considered two-channel structure can be obtained for a periodic system of alternating channels 1 and 2 equally spaced (at distance d from each other). This equation has the form

$$\frac{g_{11}}{(\omega(k)-kv)^2}+\frac{g_{12}+g_2}{\omega^2(k)} = \frac{\tanh kd}{k}\left\{1+\frac{k^2 g_2}{\omega^2(k)}\left[\frac{g_{11}}{(\omega(k)-kv)^2}+\frac{g_{12}}{\omega^2(k)}\right]\right\}, \tag{35}$$

where $g_{11,12}=e^2N_{11,12}/2\kappa_D m_1$, $g_2=e^2N_2/2\kappa_D m_2$, N_{11} and N_{12} are concentrations of traversing and nontraversing electrons in channel 1, respectively: $N_{11}+N_{12}=N_1$, $N_{1,2}$ are the electron concentrations (cm^{-2}) in channels 1 and 2, respectively (for the QRs!), m_1 and m_2 are effective masses in channels 1 and 2, and v is a traversing electron velocity in channel 1. If we assume that $g_2=\infty$ in Eq. (35), we obtain the dispersion Eq. (32) (but with new designations for electron concentrations). In the saturation regime, $g_{12}=0$ and $g_{11}=g_1$. This saturation regime occurs if a potential of the QR in channel 1 is equal to $V_{s1}=eN_{D1}d/3\kappa_D+2V_G/3$. Then we obtain in the QR

$$N_1=(1/3)N_{D1}+(2/3)(\kappa_D/ed)V_G,$$

$$N_2=N_{D2}+(2/3)N_{D1}-(2/3)(\kappa_D/ed)V_G, \tag{36}$$

where V_G is the biasing potential of channel 2 relative to the cathode (source) of channel 1, $N_{D1,2}$ are electron concentrations in channels 1 and 2, respectively, for zero voltages: $V_A=V_G=0$. We assume that all of the donors supplying electrons to the channels are ionized, and all of the electrons supplied by these donors are found only in the considered channels. At $V_G=V_{G0}=(ed/\kappa_D)(3N_{D2}+N_{D1})/4$ concentrations N_1 and N_2 are equal to each other. For the initially symmetric channels ($N_{D1}=N_{D2}=N_D$), this symmetry can be restored in the saturation regime only at the single biasing potential $V_G=edN_D/\kappa_D$. Since the concentrations $N_{1,2}$ are non-negative, the limits of V_G variations are determined by inequalities

$$-edN_{D1}/2\kappa_D<V_G<ed(3N_{D2}+2N_{D1})/2\kappa_D. \tag{37}$$

In this range, the saturation voltage V_{s1} in channel 1 varies within the limits: $0<V_{s1}<ed(N_{D1}+N_{D2})/\kappa_D$. Instead of $g_{1,2}$, we introduce two new parameters: $g_{1,2}=\overline{g}\pm\delta g$. If effective masses are the same ($m_{1,2}=m$), the value of $\overline{g}$ is determined by the summary donor concentration: $\overline{g}=e^2(N_1+N_2)/4\kappa_D m=e^2(N_{D1}+N_{D2})/4\kappa_D m$, and δg is controlled by the potential V_G: $\delta g=e^2(N_1-N_2)/4\kappa_D m=eV_G/3dm-e^2(N_{D2}+N_{D1}/3)/4\kappa_D m$. Thus Eq. (35) can be rewritten in the form

$$\xi^4-\frac{1}{2}\left(1+\frac{1}{2\zeta}\right)\xi^2-\frac{\delta g}{4\overline{g}}\frac{1}{\zeta}\xi+\frac{1}{16}\left(1-\frac{1}{\zeta}\right)-\left(1-\left(\frac{\delta g}{\overline{g}}\right)^2\right)\left(\frac{kd^*}{8\zeta}\right)^2=0, \tag{38}$$

where $\xi=\omega(k)/kv-1/2$ is the same as in Eq. (34), but now $\zeta=d^*k^2v^2/8\overline{g}$, $d^*\tanh=kd/k$. For $kd\ll 1$ we obtain $d^*\cong d$, and $\zeta=\kappa_D k^2 dV_{s1}/e(N_{D1}+N_{D2})$. Taking into account the above-mentioned limits of varying V_{s1}, we have: $0<\zeta<k^2d^2$. Equation (38) has very simple solutions for the specific case $\delta g=0$ and for $kd\ll 1$. For $\delta g=0$, we obtain the two-stream instability if $kd<1.6715$. If $k^2d^2\ll 1$ (that is, if $\zeta\ll 1$), Eq. (38) is reduced to the form

$$\xi^2+\frac{\delta g}{\overline{g}}\xi+\frac{1}{4}+\frac{1}{8}\left(1-\frac{\delta g}{\overline{g}}\right)=0 \tag{39}$$

and has complex roots for all of the values of δg. As a result, we obtain

$$\omega(k)=k\sqrt{\overline{g}d}\sqrt{1-(\delta g/\overline{g})^2}\left(\sqrt{1-\delta g/\overline{g}}\pm i\sqrt{3/2+\delta g/\overline{g}}\right). \tag{40}$$

The maximal frequency occurs not for $\delta g=0$ but for $\delta g=-1/3$. This maximal frequency does not noticeably exceed $k\sqrt{\overline{g}d}$.

V. NUMERICAL RESULTS FOR FETS

In Secs. II–IV, we have considered the dispersion equations, which describe the development of the small concentration and electrical potential fluctuations in the QRs for several versions of ungated and gated ballistic devices. The dispersion relations, obtained from these equations, allow us to reveal unstable distributions and predict oscillatory regimes. In this section we take the next step and consider some results of numerical simulations in gated ballistic base channels (that is, in FETs). These results give evidence of the two-stream instability globalization and self-organization of oscillatory regimes in high-frequency short-circuited FETs. Specifically, we simulate the asymmetric single-gate structures and specify drain and gate potentials relative to the source but we exclude any load elements in both the drain–source and the gate–source loops. This means that the con-

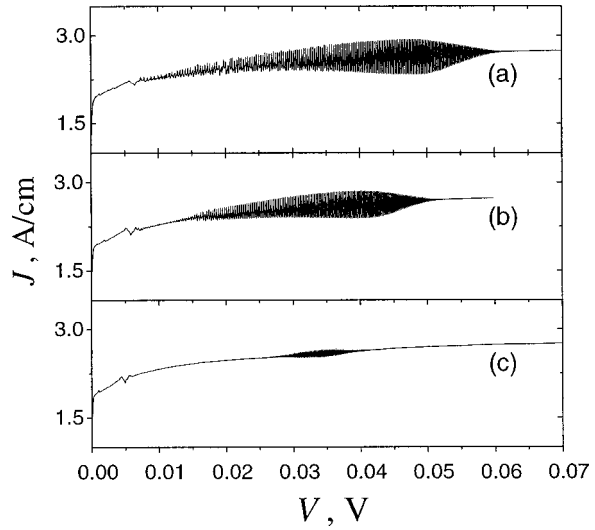

FIG. 5. *JV* characteristics with oscillatory sections for three short FETs with different channel lengths: (a) $l=0.175$ μm; (b) $l=0.15$ μm; (c) $l=0.125$ μm.

sidered oscillatory regimes are incompletely optimized. What is more, in some cases when the above-mentioned globalization is not reached, it can be obtained by selecting a certain optimal reactive load.

The FETs are subjects of special interest to us because the gates transform the appearing instability into the absolute form. This absolute instability does not lead directly to any oscillatory regimes. But on the other hand, we have already had some results of studying the two-stream instability in FETs,[13] and they undoubtedly demonstrate oscillatory regimes.

In Fig. 5, we demonstrate drain currents J versus drain–source voltages V for three short FET ''samples'' with channel lengths $l=0.175$, 0.15, and 0.125 μm. Gate lengths are shorter: $l_G=0.8l=0.14$, 0.12 and 0.1 μm, respectively. The channel electron gas is two-dimensional and has a high initial concentration $N=N_D+\kappa_D V_G/ed$, where $N_D=4\times10^{11}$ cm^{-2}, $V_G=30$ mV, and $d=16$ nm. The source and drain contacts are asymmetrical: $\mu_S=0.06$ eV, $\mu_D=0.015$ eV, where $\mu_{S,D}$ are the Fermi energies of electrons that entered the channel from the source and the drain, respectively. The electron effective mass is equal to $m=0.067m_0$, where m_0 is the free electron mass. Electron conductivity in the barriers is assumed to be absent. All the other details of the simulation procedure are the same as in the previous work[13] devoted to ballistic FETs with negative-effective-mass carriers in the channel. We see in Fig. 5 that the voltage sections of current oscillations are wider for longer bases and narrower for shorter bases, and current oscillation amplitude is greater in longer bases. But an oscillation frequency is higher just in shorter bases. These results correspond completely to the well-known general tendency but they cannot be predicted in the above-described picture of instability based on the extended QR.

Distributions of electron concentration and electric potential in the base of the $l=0.175$ μm sample are depicted in Fig. 6 for three values of $V=10$, 47, and 64 mV. The smallest value corresponds to the lower boundary of the oscillation interval, the greatest one corresponds to the upper boundary, and the intermediate value corresponds to the maximal oscillation amplitude. We can make sure that the QR does really occupy a substantial part of the gated base

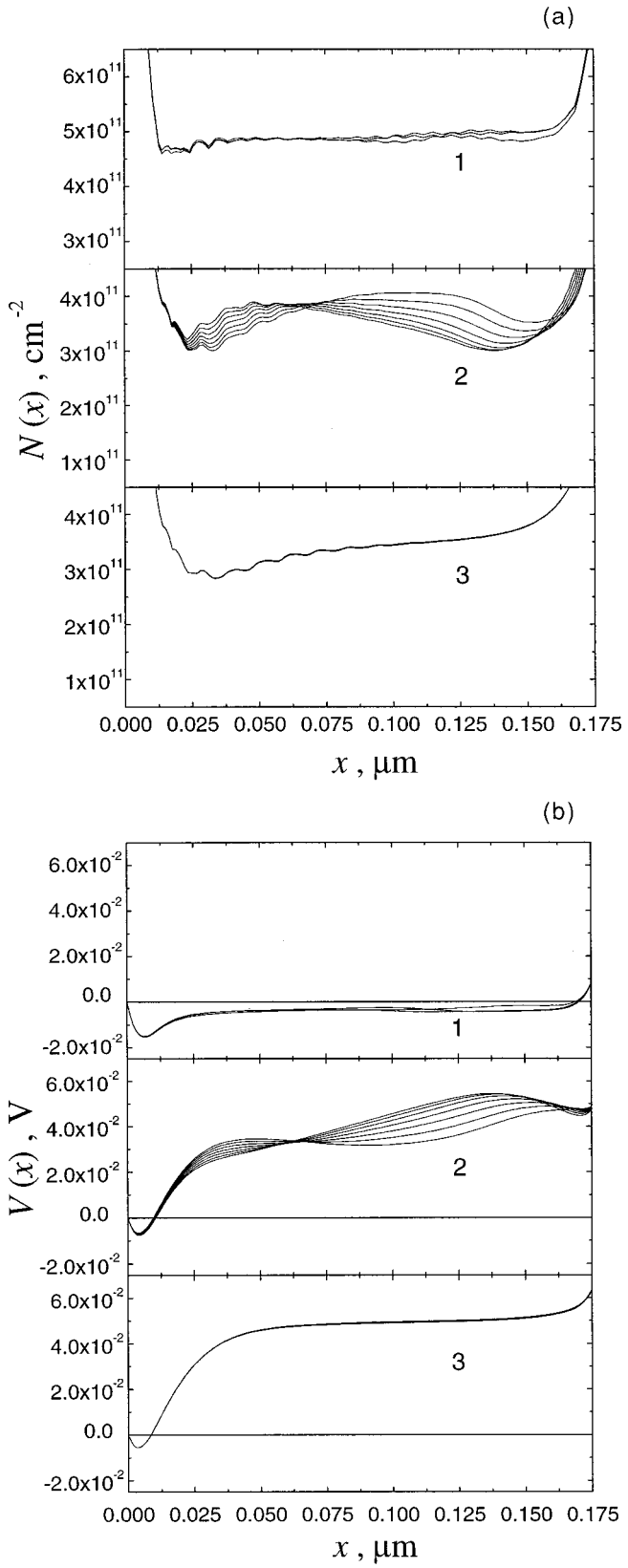

FIG. 6. Distributions of electron concentration $N(x)$ (a) and electric potential $V(x)$ (b) for three values of the drain-source voltage V: (1) $V=10$ mV; (2) $V=47$ mV; (3) $V=64$ mV; $l=0.175$ μm [sample (a) in Fig. 5].

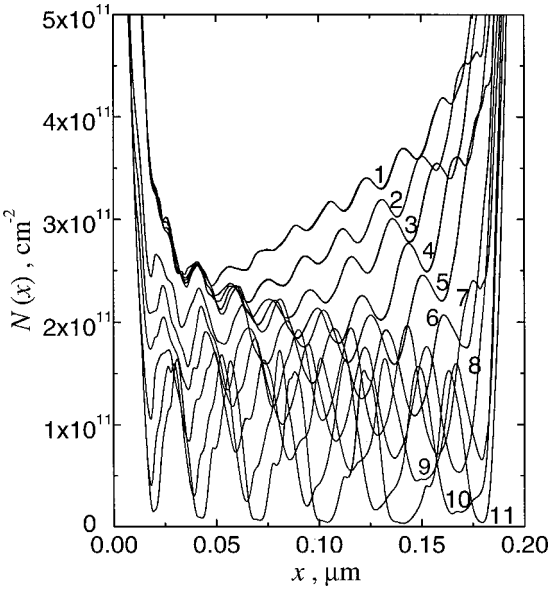

FIG. 7. Quasiperiodic concentration nonmonotonicities in the FET with a heavily doped channel and a wide gate-channel barrier; $V_G=30$ mV, $V=0.25$ V (1); 0.27 V (2); 0.3 V (3); 0.35 V (4); 0.42 V (5); 0.53 V (6); 0.63 V (7); 0.75 V (8); 1.0 V (9); 1.4 V (10); 1.75 V (11).

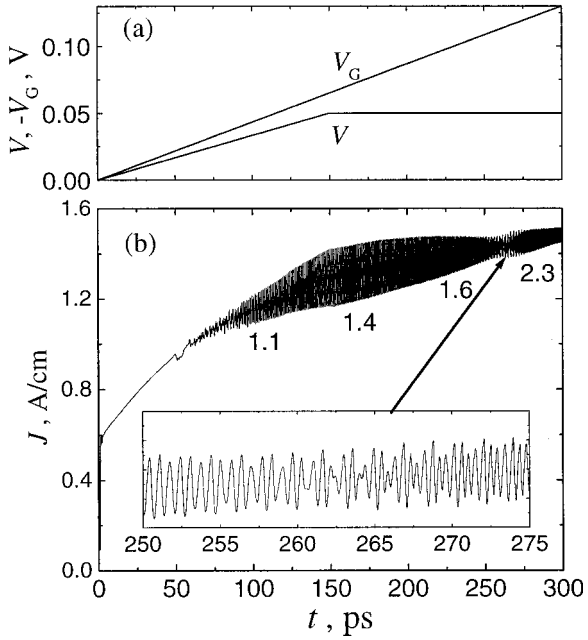

FIG. 8. Gate potential control of an oscillation frequency for the ballistic FET with parameters: $l=0.35$ μm, $l_G=0.28$ μm, $N_D=2\times10^{11}$ cm^{-2}, $\mu_F^{(S)}=0.035$ eV, $\mu_F^{(D)}=0.0175$ eV. Other parameters are the same as in the samples in Fig. 5. (a) V_G and V vs time t; (b) J vs time t; numbers under the curve in (b) show oscillation frequency in THz.

section. The concentration and potential oscillations contain the additional (intermediate) node at $x_N=0.063$ μm along with the boundary nodes at the source and the drain. It seems that this intermediate node separates the gated space into the source–gate current and the drain–gate current zones.

Some quasiperiodic concentration nonmonotonicities (QCNs) attract our attention in the concentration distributions in Fig. 6. They take place in stationary pictures (before and after oscillation regimes) and in nonstationary pictures (during these oscillations). These QCNs are incompletely stable: their positioning and periodicity are sensitive to different details of the numerical procedure (for example, to mesh sizes in real and momentum spaces). However, we cannot remove these nonmonotonicities completely. To study evolution of such QCNs, we have ''prepared'' a special sample ($l=0.2$ μm) with a heavy doping ($N_D=5\times10^{11}$ cm^{-2}) and a wide barrier between the channel and the gate ($d=48$ nm). The current in this sample saturates at very high voltages. The concentration distributions in this sample are shown in Fig. 7. For several values of V (beginning with $V=0.25$ V and right up to 1.0 V), stable distributions in the form of wide and deep strata appear. Unlike the small stratification in Fig. 6, this stratification has not been subjected to the influence of the above mentioned details of the numerical procedure. It is accompanied by stationary current oscillations depending on the drain–source voltage V. There appears the I–V characteristic with repeated negative differential conductivity sections without any marks of high-frequency current oscillations. We suppose that the picture of concentration stratification shown in Fig. 7 is a result of the development of the absolute instability mentioned in Sec. III B. This very pronounced stratification blocks any possibility of a high-frequency oscillatory regime. We also suppose that the small stratification ripples in Fig. 6 are caused by the same absolute instability. In this case, the concentration distributions are very multivalued and determined by small inner inhomogeneities (including the ones contributed by the numerical digital procedure). Such small stratification does not impede development of the convective instability and the oscillatory regime formation. We can see this process in Fig. 6. This means that the oscillatory regimes are possible if the stratification is not very pronounced.

To complete the picture, we mention that we have repeatedly observed small concentration stratification under our numerous simulations of the two-stream instability development in various structures, which are not described here. This small stratification occurs not only in gate-based channels but also in ungated-channel-based structures and in bulk-based diodes. As a rule, such small stratification occurs either in short bases or in short contact-adjacent sections of longer bases. The concept of absolute and convective instability introduced for infinite medium becomes invalid in these cases.

A frequency of oscillations generated as a result of the two-stream instability in the FET can be tuned in a wide range by the gate potential. In Fig. 8 we demonstrate a twofold increase in oscillation frequency due to enhancing gate potential V_G for the same V. This increase can be still greater in other samples.

The numerical results presented here are of model nature and aim to describe the qualitative picture of two-stream instability development in the short bases with ballistic electron transport. The specified simulation of possible terahertz generators requires detailed estimation of realistic ranges of the base doping, length, and the voltages V_G and V.

VI. DISCUSSION AND CONCLUDING REMARKS

We have shown above that without fast electron–electron mixing in the momentum space, ballistic electron transport leads to a two-stream electron distribution function in short diode and FET bases. In its turn, the two-stream distribution function induces two-stream instability, due to a strong interaction of plasma oscillations in each of the streams. We have considered dispersion relations $\omega(k)$ of small two-stream plasma oscillations for the bulk, ungated channel, gated channel (FET), and two-channel bases (in the cold stream approximation). The instability of stationary streams is shown in all of these cases. The instability is convective for the extended bulk and ungated-channel bases and absolute for the gated-channel (FET) bases. Despite the indicated distinction, the completed numerical simulations have displayed oscillatory regimes for all these cases. We can present two nonconflicting explanations of this phenomenon. (1) The absolute instability only leads to a small-scale stratification, which cannot impede the development of a large-scale convective instability in a small-scale-stratified medium. (2) Some of our numerical simulations are completed for bases that are too short, and categories of the absolute and convective instabilities are not justified in these bases.

Devices based on two-stream instability have several noticeable advantages in comparison with the negative-effective-mass (NEM) diodes and FETs, considered in Refs. 13, 14, and 29 and suggested as terahertz range generators. All of the NEM mechanisms are specific and cause additional technology problems [p-type quantum well (QW),[13,14] asymmetric double QW,[30] combined ΓX-QW,[30] etc]. Two-stream instability does not require any peculiarities in the electron dispersion relation. It can develop in both 2D and 3D electron gases. Specifically, electrons in quasitriangular modulation-doped single-heterojunction QWs are well suitable for this aim. (Note that in this case maximal mobility and mean free path can be reached.) But two-stream instability is very sensitive to pair electron–electron interaction between the streams. We cannot boost an electron concentration because scattering time τ_{12} decreases as n^{-2} for bulk bases and as $(N^2 \ln N)^{-1}$ for channels with 2D electron gas.[16–18] This inability to increase the concentration does not allow shortening of the base length. We also cannot increase the accelerated stream velocity because scattering time τ_{12} decreases with increase in this velocity. This means that any hopes of adapting the two-stream instability to sufficiently high temperatures ($\gg 10-20$ K) are illusive. (Note in this connection, that the NEM mechanism is indifferent to pair electron–electron interaction. Adaptation of the NEM instability for elevated temperatures is limited by the absence of real NEM mechanisms with the NEM section energy greater than 0.03–0.05 eV).

As we have noted in Secs. I and IV, the pair electron–electron interaction can be significantly suppressed by spatial separation of the streams into two independent channels. One of these channels (for example, the channel with $v=0$) could contain a hole gas. Such a two-channel structure is similar to the device described in Ref. 27. In this case a voltage across the interchannel barrier enhances carrier concentrations in both channels simultaneously (instead of the electron redistribution considered in Sec. IV). As a result, the voltage control can be much more effective in comparison with the case of channels of the same type of conductivity.

ACKNOWLEDGMENTS

The authors thank Dr. D. Romanov for fruitful discussion, and Peggy Heine and Olga Melnikova for numerous valuable notations. This work is supported by a NSF grant.

[1] J. R. Pierce, J. Appl. Phys. **19**, 231 (1948).
[2] M. V. Nezlin, Sov. Phys. Usp. **11**, 608 (1971).
[3] M. C. Steel and B. Vural, *Wave Interactions in Solid State Plasmas* (McGraw–Hill, New York, 1969).
[4] Yu. K. Pozhela, *Plasma and Current Instabilities in Semiconductors* (Nauka, Moscow, 1977).
[5] B. B. Robinson and G. A. Swartz, J. Appl. Phys. **38**, 2461 (1967).
[6] G. A. Swartz and B. B. Robinson, J. Appl. Phys. **40**, 4598 (1969).
[7] N. A. Bannov, V. I. Ryzhii, and V. A. Fedirko, Sov. Phys. Semicond. **17**, 36 (1983).
[8] V. I. Ryzhii, N. A. Bannov, and V. A. Fedirko, Sov. Phys. Semicond. **18**, 481 (1984).
[9] Z. S. Gribnikov and A. N. Korshak, Semiconductors **28**, 812 (1994).
[10] A. A. Sukhanov, V. B. Sandomirskii, and Yu. Yu. Tkach, Sov. Phys. Semicond. **17**, 1378 (1983).
[11] V. V. Mantrov and A. A. Sukhanov, Sov. Phys. Semicond. **19**, 882 (1985).
[12] E. M. Lifshitz and L. P. Pitaevski, *Physical Kinetics*, edited by L. D. Landau and E. M. Lifshitz, Course of Theoretical Physics, Chap 10 (Pergamon, Oxford, 1980).
[13] Z. S. Gribnikov, N. Z. Vagidov, A. N. Korshak, and V. V. Mitin, J. Appl. Phys. **87**, 7466 (2000).
[14] Z. S. Gribnikov, A. N. Korshak, and V. V. Mitin, Int. J. Infrared Millim. Waves **20**, 213 (1999).
[15] R. J. Briggs, *Electron-Stream Interactions with Plasmas* (MIT Press, Cambridge, MA, 1964).
[16] V. F. Gantmakher and Y. B. Levinson, *Carrier Scattering in Metals and Semiconductors* (North-Holland, Amsterdam, 1987).
[17] A. V. Chaplik, Sov. Phys. JETP **33**, 997 (1971).
[18] G. F. Guiliani and J. J. Quinn, Phys. Rev. B **26**, 4421 (1982).
[19] M. Artaki and K. Hess, Phys. Rev. B **37**, 2933 (1988).
[20] G. Fasol, Appl. Phys. Lett. **59**, 2430 (1991).
[21] F. Müller, B. Lengeler, Th. Schäpers, J. Appenzeller, A. Förster, Th. Klocke, and H. Lüth, Phys. Rev. B **51**, 5099 (1995).
[22] Th. Schäpers, M. Krüger, J. Appenzeller, A. Förster, B. Lengeler, and H. Lüth, Appl. Phys. Lett. **66**, 3603 (1995).
[23] P. J. Price, Physica B & C **117B & 118B**, 750 (1983).
[24] C. Jacoboni and P. J. Price, Solid-State Electron. **31**, 649 (1988).
[25] B. Laikhtman and P. M. Solomon, Phys. Rev. B **41**, 9921 (1990).
[26] P. M. Solomon, P. J. Price, D. J. Frank, and D. C. La Tulipe, Phys. Rev. Lett. **63**, 2508 (1990).
[27] U. Sivan, P. M. Solomon, and H. Shtrikman, Phys. Rev. Lett. **68**, 1196 (1992).
[28] T. J. Gramila, J. P. Eizenstein, A. H. MacDonald, L. N. Pfeiffer, and K. W. West, Phys. Rev. Lett. **66**, 1216 (1991).
[29] A. N. Korshak, Z. S. Gribnikov, N. Z. Vagidov, and V. V. Mitin, Appl. Phys. Lett. **75**, 2292 (1999).
[30] Z. S. Gribnikov, A. N. Korshak, and N. Z. Vagidov, J. Appl. Phys. **80**, 5799 (1996).